Acta Crystallographica Section D
**Biological Crystallography**
ISSN 0907-4449

# Structure of bovine adenosine deaminase complexed with 6-hydroxy-1,6-dihydropurine riboside

**Takayoshi Kinoshita,[a]* Nobuya Nishio,[a] Isao Nakanishi,[a] Akihiro Sato[b] and Takashi Fujii[a]**

[a]Exploratory Research Laboratories, Fujisawa Pharmaceutical Co. Ltd, 5-2-3 Tokodai, Tsukuba, Ibaraki 300-2698, Japan, and [b]Analytical Research Laboratories, Fujisawa Pharmaceutical Co. Ltd, Kashima 2-1-6, Yodogawa-ku, Osaka, 532-8514, Japan

Correspondence e-mail: takayoshi_kinoshita@po.fujisawa.co.jp

Received 15 January 2002
Accepted 26 November 2002

**PDB Reference:** ADA–HDPR complex, 1krm, r1krmsf.

The crystal structure of adenosine deaminase (ADA) from bovine intestine complexed with a transition-state analogue, 6-hydroxy-1,6-dihydropurine riboside (HDPR), was solved at 2.5 Å resolution by the molecular-replacement method using a homology model based on the crystal structure of mouse ADA. The final refinement converged to a crystallographic $R$ factor of 20.7%. The $C^{\alpha}$ backbone of bovine ADA is mostly superimposable on that of mouse ADA, although mouse ADA itself did not lead to a solution by molecular replacement. HDPR tightly interacts with ADA by means of six hydrogen bonds and is entirely enclosed within the active site. The lid of the envelope consists of two components: one contains two leucine residues, Leu55 and Leu59, and the other contains the backbone atoms Asp182 and Glu183. The $C^{\delta}$ atoms of the two leucine residues are 3.5 Å from the respective N atoms of the backbone. A weak interaction, similar to CH–$\pi$ binding, might make it possible to open the lid. Taking account of the movement and observation of this structural feature, the aim is to design novel ADA inhibitors.

## 1. Introduction

Adenosine deaminase (ADA; EC 3.5.4.4) catalyzes the irreversible deamination of both adenosine and deoxyadenosine to inosine and deoxyinosine, respectively. ADA is one of the enzymes involved in the purine pathway and is distributed in most mammalian tissues. It is indispensable to the upkeep of a competent immune system, as heritable ADA deficiency is associated with severe combined immunodeficiency disease (SCID; Martin & Gelfand, 1981). ADA has also been shown to be involved in T-cell activation (Kameoka *et al.*, 1993). Both enzyme-replacement therapy (Levy *et al.*, 1988) and gene therapy (Marshall, 1995) have been used to treat victims of this rare disease. On the other hand, elevated ADA levels are associated with a number of diseases and ADA inhibitors have seen clinical usage as antimetabolic and antineoplastic agents and as modulators of neurological function through their effects on adenosine levels (Glazer, 1980; Centelles et al., 1988). However, these drugs are seldom used because of severe toxicity resulting from the fact that all known inhibitors are nucleoside analogues. Therefore, toxicity-free drugs would be a major and significant improvement.

For the purpose of the discovery of improved drugs, structure-based drug design (SBDD) with the aim of the discovery of non-nucleoside inhibitors may be most effective. As the first step of SBDD, we planned to examine human ADA by X-ray analysis; however, sufficient quantities of human ADA are difficult to obtain. We thus decided to examine bovine ADA, although all X-ray studies to date on ADA have been carried out using mouse ADA (Wilson *et al.*,

1991, 1993; Sharff *et al.*, 1992; Sieraki, Mohamedali *et al.*, 1996; Sieraki, Wilson *et al.*, 1996).

Of the known ADA amino-acid sequences, bovine ADA is the closest to human ADA. Furthermore, bovine ADA derivatized with polyethylene glycol (Hershfield *et al.*, 1987) has been administered to replace deficient human ADA. This means that human and bovine ADA are very close to each other and are functionally interchangeable. The amino-acid sequences of human and bovine ADA are 91% homologous (Wiginton *et al.*, 1984; Kelly *et al.*, 1996). Bovine and mouse ADA (Yeung *et al.*, 1985) are 85% homologous and human and mouse ADA are 83% homologous, respectively. In particular, the amino-acid residues around the active sites of human and bovine ADA are completely identical.

Furthermore, it is suggested that the active sites of bovine ADA and human ADA are different from that of mouse ADA, as a single mutation is present at a structurally important site, namely at the end of the movable component of the active-site cleft. ADA has a common structural motif: a TIM barrel which contains a parallel $\alpha/\beta$-barrel motif with eight central $\beta$-strands and eight helices and which has movable components on the top of the barrel. These types of component often move greatly if an inhibitor or substrate binds to the active site. For example, aldose reductase and triosephosphate isomerase have different conformations as a result of inhibitor-induced fitting when inhibitors bind (Harrison *et al.*, 1997; Mande *et al.*, 1994).

We believe that precise observation of the structural features of bovine ADA may lead to the design of novel non-nucleoside-type inhibitors owing to its functional and structural similarity to human ADA. In this paper, the crystal structure of bovine ADA complexed with HDPR is described.

**Table 1**
Data-collection and refinement statistics of bovine ADA complexed with HDPR.

Values in parentheses are for the highest resolution shell.

| | |
|---|---|
| Data collection and processing | |
| Space group | $P4_32_12$ |
| Unit-cell parameters (Å) | $a$ = 79.19, $c$ = 141.62 |
| Diffraction data | |
| Resolution (Å) | 30.0–2.5 (2.59–2.50) |
| Unique reflections | 16108 |
| $R_{sym}$ (%) | 5.0 (18.7) |
| Completeness (%) | 99.2 (100.0) |
| Redundancy | 8.9 (7.9) |
| $I/\sigma(I)$ (overall) | 10.5 (3.4) |
| Refinement | |
| $R_{cryst}/R_{free}$ (%) | 20.7/24.1 |
| Final model | |
| Protein residues | 349 |
| $Zn^{2+}$ | 1 |
| HDPR | 1 |
| Water | 222 |
| R.m.s. deviations | |
| Bonds (Å) | 0.007 |
| Angles (°) | 1.6 |
| Dihedrals (°) | 24.3 |
| Impropers (°) | 0.83 |
| Mean $B$ factor (Å$^2$) | |
| Protein | 42.9 |
| $Zn^{2+}$ | 26.6 |
| HDPR | 27.9 |
| Water | 56.9 |
| All | 43.9 |

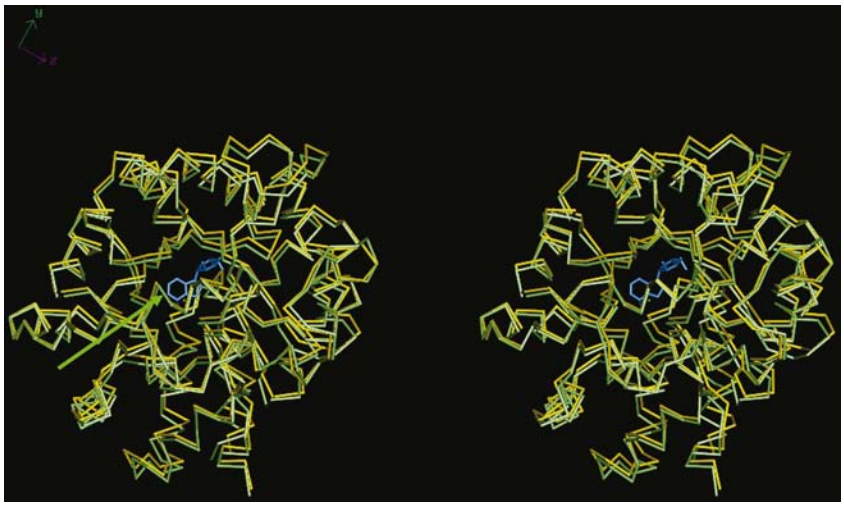

**Figure 1**
Stereoview of superimposed $C^{\alpha}$ backbone structures of the complex with HDPR (white, bovine holoenzyme; yellow, mouse holoenzyme; blue, HDPR). The two holoenzyme molecules have almost the same backbones. A critical mutation is located at the top of the active site (green arrow).

## 2. Methods and results

### 2.1. Crystallization and data collection

ADA from bovine intestine was purchased from Roche Diagnostics Inc. and purine riboside was purchased from Sigma. The crystals of the complex used for data collection were grown against reservoirs containing 2.0–2.2 *M* ammonium sulfate, 2%(*v*/*v*) polyethylene glycol 400 in 0.1 *M* HEPES buffer pH 7.5. The crystals grew to maximum dimensions of approximately 0.3 × 0.2 × 0.15 mm in two weeks. The details of the crystallization have been described previously (Kinoshita *et al.*, 1999).

After dipping a crystal in a solution of Paratone-N (Hampton Research Inc.), X-ray diffraction data were collected at 100 K using a Rigaku R-AXIS V imaging-plate system at beamline BL24XU of the SPring-8 facility (Harima, Japan). The crystal-to-imaging plate distance was 300 mm and the oscillation range was 1°, with an exposure time of 30 s. 150 frames of data were collected. The space group was assigned as $P4_12_12$ or $P4_32_12$, with unit-cell parameters $a = b = 80.03$, $c = 141.68$ Å. Data processing was performed using the program *Crystal Clear* (Rigaku). The data-collection statistics for the data set are summarized in Table 1.

### 2.2. Structure determination

The structure of the complex was solved by the molecular-replacement technique using the program *AMoRe* from the *CCP*4 program

suite (Navaza, 1994; Collaborative Computational Project, Number 4, 1994). At first, the structure of mouse ADA (PDB code 1add; Wilson *et al.*, 1991) was directly used as a search model. However, this attempt did not lead to a clear solution. Therefore, a model of bovine ADA was used as a search model. This homology model was constructed based upon the crystal structure of mouse ADA using the *SYBYL* molecular-modelling software (Tripos Inc). The model was energetically minimized to avoid illegal contacts. The rotation function successfully afforded a clear solution. Subsequently, a clear solution of the translation function was obtained in the case of space group $P4_32_12$ and no illegal contacts in the crystal were detected. Furthermore, the electron density of the helix part showed a precise $\alpha$-helix. Thus, the space group of the crystal was confirmed as $P4_32_12$. The $R$ factor after initial rigid-body refinement using 8.0–4.0 Å resolution data was 34.2%.

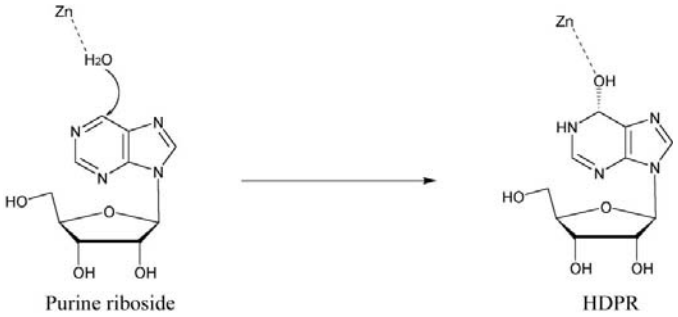


**Figure 2**
Diagram showing the conversion of the inhibitor. Purine riboside is converted to the 6-hydroxy derivative HDPR. In native ADA, an activated water is ligated to zinc. This water near the compound attacks the substrate (or inhibitor) in the vertical direction.

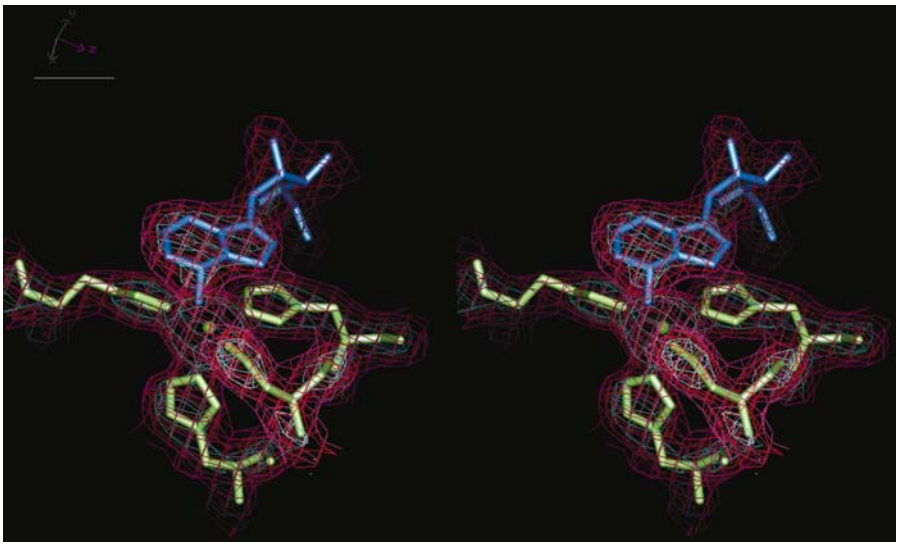

**Figure 3**
Stick models of HDPR (blue) and four amino acids (white) and a sphere model of zinc (green). The models are enclosed in the wire-cage representation of the electron-density map calculated at 2.5 Å resolution by a Fourier transform using $2|F_o| - |F_c|$ coefficients (pink, $1\sigma$ level; orange, $2\sigma$ level; grey, $3\sigma$ level). $F_c$ values were calculated from the final protein structure without HDPR. The electron density is continuous from the hydroxyl group in the C-6 axial position of the purine riboside to the zinc ion. The side chains of three histidine residues and an asparagine residue on the top of the TIM barrel also make coordination bonds to the zinc ion.

After a subsequent rigid-body refinement at 2.5 Å resolution, HDPR was easily placed in the $2\sigma$-level envelope of the $F_{obs} - F_{calc}$ difference map. Subsequently, refinement with all data was performed using the *CNX* package (Accerlys Inc.) using torsion-angle dynamics and individual $B$-factor refinement. A randomly selected 5% of the data set was set aside for cross-validation using the $R_{free}$ value and bulk-solvent correlation was used. During the refinement, solvent molecules were progressively added when they met the following requirements: (i) a minimum $3\sigma$ peak had to be present in the $F_{obs} - F_{calc}$ difference map, (ii) a peak had to be visible in the $2F_{obs} - F_{calc}$ map, (iii) the $B$ value for the water molecule should not exceed 80 Å$^2$ during refinement and (iv) the water molecules had to be stabilized by hydrogen bonding. Visual inspection and model building were performed using *QUANTA* (Accerlys Inc.).

## 3. Results and discussion

The $C^\alpha$ backbone traces of bovine and mouse ADA are very close to each other, with an r.m.s.d. value of 0.57 Å (Fig. 1), although mouse ADA did not lead to a perfect solution using molecular replacement. The reason may be that different crystal packing results in a slight but significant conformational change. Generally, modification of the starting model, such as a polyalanine model or an omit-model without outer region loops, can lead a clear solution. However, the bovine ADA model was easily constructed itself, rather than by modification of mouse ADA; therefore, the bovine ADA model was used as a start model. The main structural architecture of bovine ADA, the so-called TIM barrel, remained. Two amino acids from the N-terminus and five from the C-terminus were omitted from the final model because of ambiguous or discontinuous electron density for the corresponding regions. Furthermore, the C-terminus and N-terminus in the final model lay in the solvent region and the $B$-factor values of the corresponding $C^\alpha$ atoms are high compared with the average (Thr1, 65.6 Å$^2$; Arg349, 70.3 Å$^2$; average, 42.9 Å$^2$). However, the two termini of ADA are considered irrelevant to drug design since they are far removed from the putative active site.

Purine riboside was used as an inhibitor in the preparation of the complex solution and was converted to HDPR, a hydroxy derivative, by ADA during crystallization (Fig. 2). Subsequently, HDPR remained at the active site and formed a coordination bond with zinc, although the substrate adenosine is converted to inosine, a hydroxy derivative, which then leaves the active site. The electron density of the inhibitor quite

clearly continued from the hydroxyl group in the axial C-6 position of the purine-ring system to the zinc ion (Fig. 3). The hydroxyl group is one of the five ligands and the distance between the zinc ion and hydroxyl group of HDPR is 2.1 Å. In the native structure, an activated water molecule coordinates to the zinc ion in place of the hydroxyl group. In addition to the hydroxyl group, the zinc ion is also coordinated by His12 $N^{\varepsilon}$ (2.2 Å), His14 $N^{\varepsilon}$ (2.1 Å), His211 $N^{\varepsilon}$ (2.2 Å) and Asp292 $O^{\delta1}$ (2.3 Å). HDPR also tightly interacts with ADA by means of six hydrogen bonds (Fig. 4). The N-1 atom of the purine ring makes a hydrogen bond with Glu214 $O^{\varepsilon}$ (2.9 Å), the N-3 atom with Gly181 NH (3.0 Å), the N-7 atom with Asp293 $O^{\delta}$ (2.8 Å), the 6-hydroxyl group with Asp292 $O^{\delta}$ (2.7 Å), the 5′-hydroxyl group with His14 $N^{\varepsilon}$ (2.9 Å) and the 3′-hydroxyl group with Asp16 $O^{\delta}$ (2.5 Å). HDPR also forms a hydrogen bond directly with a water molecule in the hydrocarbon part, where water is located, and this closes the entrance of the active site. The 2′-hydroxyl and 3′-hydroxyl groups interact with water 569 (2.7 and 2.8 Å, respectively).

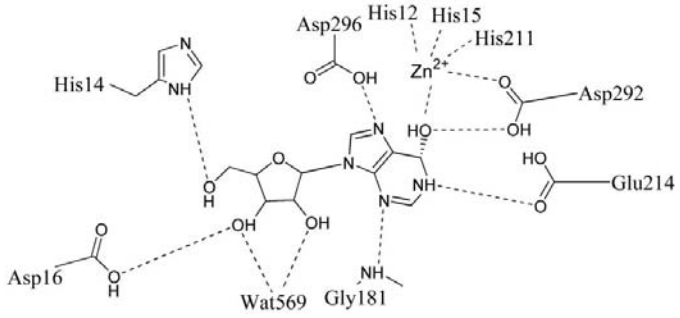


**Figure 4**
Interaction mode between ADA and HDPR. The dotted lines show hydrogen bonds and coordination bonds. HDPR interacts with ADA *via* six direct hydrogen bonds and with zinc *via* a coordination bond. Only a water molecule interacts with HDPR *via* two hydrogen bonds.

Bound HDPR occupies almost the entire active-site cavity at the top of the $\beta$-barrel. The bound inhibitor is almost buried in the active site and has an accessible surface area of 8.5 $Å^2$, 3.4% of the total surface area of the unbound inhibitor (Fig. 5). Therefore, it is necessary for ADA to undergo conformational change at the active site when the inhibitor or substrate binds or leaves, since the compounds cannot leave through the narrow hole around the hydrocarbon moiety of HDPR. The lid of the envelope consists of two components: one contains two leucine residues and the other contains the backbone of the opposite side. Leu55 $C^{\delta1}$ interacts perpendicularly with the peptidyl N atom of Asp182. Similarly, Leu59 $C^{\delta2}$ interacts with the peptidyl N atom of Glu183. Both $C^{\delta}$ atoms of the two leucine residues are 3.5 Å from the respective N atoms of the backbone. These weak interactions, which are similar to CH–$\pi$ interactions, might make it possible to open the lid. However, mobility of components in the crystals was not detected. In the crystal, the movable components of both types of ADA are stabilized owing to inhibitor binding. In fact, the *B* factors of the individual atoms of the two components are almost equivalent to the average value of all protein atoms in both ADA molecules.

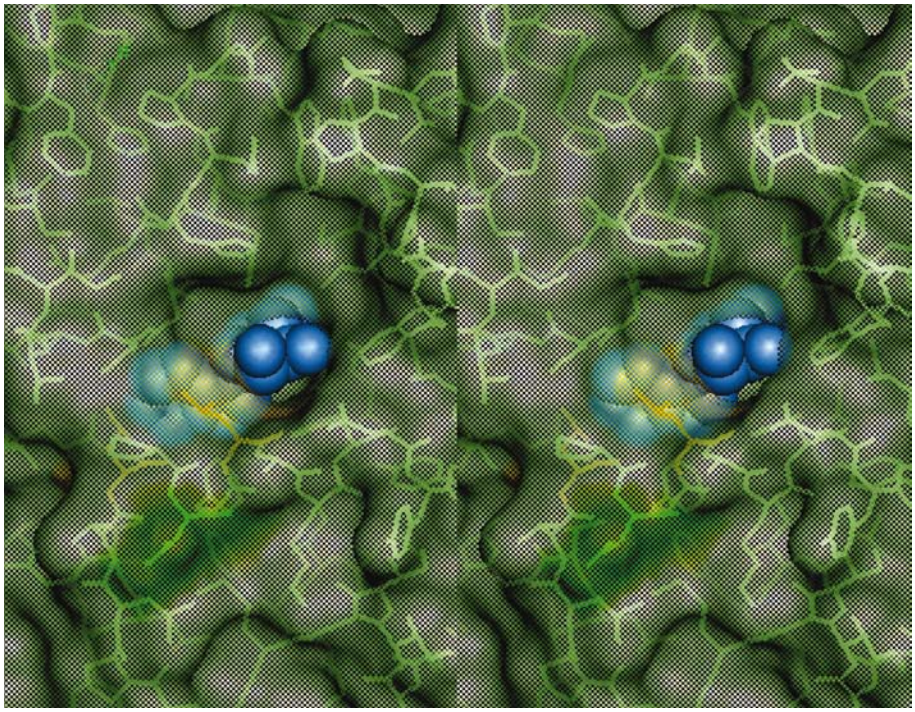

**Figure 5**
Stereoview of the movable lid. Two leucine residues (yellow) interact with the backbone N atom in the vertical direction. The interaction mode is similar to a CH–$\pi$ interaction. Both terminal C atoms are 3.5 Å from the N atoms. The mutation site (green) is located between the significant two leucine residues. Bound HDPR (blue sphere model) is almost buried in the active site.

In conclusion, bovine and mouse ADA complexed with HDPR have similar conformations and are particularly similar around the active site, in spite of a mutation between the two significant leucine residues. The interaction pattern between bovine ADA and HDPR is similar to that of mouse ADA. Therefore, it can be predicted that human ADA acts in the same way as bovine and mouse ADA. This result should be useful for structure-based drug design based upon substrate analogues such as HDPR. Nevertheless, this result does not confirm that this conformation is the only stable form or that it is one of the inhibitor-induced conformations, since HDPR cannot bind to ADA without movement of the lid on top of the active site. In practice, bovine ADA could not be crystallized in the native form under the conditions described in this paper and crystallization of mouse ADA in the native form has not yet been reported. This means that it is probably difficult to obtain the native form and that native ADA might have a number of different conformations in solution. Taking account of the movement as well

as the precise observation of the structural features, we are planning to design more effective ADA inhibitors.

We would like to thank Dr D. Barrett, Medicinal Chemistry Research Laboratories for helpful discussions and critical evaluation of the manuscript.

## References

Brünger, A. T. (1992). *X-PLOR Version 3.1: A System for X-ray Crystallography and NMR*. New Haven, CT, USA: Yale University Press.

Centelles, J. J., Franco, R. & Bozal, J. (1988). *J. Neurosci. Res.* **19**, 258–267.

Collaborative Computational Project, Number 4 (1994). *Acta Cryst.* D**50**, 760–763.

Glazer, R. (1980). *Reviews on Drug Metabolism and Drug Interactions*, Vol. 3, pp. 105–128. London: Freund Publishing House.

Harrison, D. H. T., Bohren, K. M., Petsko, G. A., Ringe, D. & Gabbay, K. H. (1997). *Biochemistry*, **36**, 16134–16140.

Hershfield, M. S., Buckley, R. H., Greenberg, M. L., Molten, R., Schiff, R., Hatem, C., Kurtzberg, J., Markert, M. L., Kobayashi, A. L. & Abuchowski, A. (1987). *N. Engl. J. Med.* **316**, 589–596.

Kameoka, J., Tanaka, T., Nojima, Y., Schlossman, S. F. & Morimoto, C. (1993). *Science*, **261**, 466–469.

Kelly, M. A., Vestling, M. M., Murphy, C. M., Hua, S., Sumpter, T. & Fenselau, C. (1996). *J. Pharm. Biomed. Anal.* **14**, 1513–1519.

Kinoshita, T., Nishio, N., Sato, A. & Murata, M. (1999). *Acta Cryst.* D**55**, 2031–2032.

Levy, Y., Hershfield, M. S., Fernandez-Mejia, C., Polmar, S. H., Scudiery, D., Berger, M. & Sorensen, R. U. (1988). *J. Pediatr.* **113**, 213–317.

Mande, S. C., Mainfroid, V., Kalk, K. H., Goraj, K., Martial, J. A. & Hol, W. G. J. (1994). *Protein Sci.* **3**, 810–821.

Marshall, E. (1995). *Science*, **267**, 1588.

Martin, D. W. Jr & Gelfand, E. W. (1981). *Annu. Rev. Biochem.* **50**, 845–877.

Navaza, J. (1994). *Acta Cryst.* A**50**, 157–163.

Sharff, A. J., Wilson, D. K., Chang, Z. & Quiocho, F. A. (1992). *J. Mol. Biol.* **226**, 917–921.

Siederaki, V., Mohamedali, K. A., Wilson, D. K., Chang, Z., Kellems, R. E., Quiocho, F. A. & Rudolph, F. B. (1996). *Biochemistry*, **35**, 7862–7872.

Siederaki, V., Wilson, D. K., Kurz, L. C., Quiocho, F. A. & Rudolph, F. B. (1996). *Biochemistry*, **35**, 15019–15028.

Wiginton, D. A., Adrian, G. S. & Hutton, J. J. (1984). *Nucleic Acids Res.* **12**, 2439–2446.

Wilson, D. K. & Quiocho, F. A. (1993). *Biochemistry*, **32**, 1689–1694.

Wilson, D. K., Rudolph, F. B. & Quiocho, F. A. (1991). *Science*, **252**, 1278–1284.

Yeung, C. Y., Ingolia, D. E., Rot, D. B., Shoemaker, C., Al-Ubaidi, M. R., Yen, J. Y., Ching, C., Bobonis, C., Kaufman, R. J. & Kellems, R. E. (1985). *J. Biol. Chem.* **260**, 10299–10307.